Electrochimica Acta 169 (2015) 462–469

Contents lists available at ScienceDirect

Electrochimica Acta

journal homepage: www.elsevier.com/locate/electacta

Multicore-shell carbon-coated lithium manganese phosphate and lithium vanadium phosphate composite material with high capacity and cycling performance for lithium-ion battery

Jia-feng Zhang [a,b], Xiao-wei Wang [b], Bao Zhang [b], Chun-li Peng [b], Hui Tong [b,*], Zhan-hong Yang [a]

[a] School of Chemistry and Chemical Engineering, Central South University, Changsha 410083, PR China
[b] School of Metallurgy and Environment, Central South University, Changsha 410083, PR China

ARTICLE INFO

Article history:
Received 2 February 2015
Received in revised form 10 March 2015
Accepted 13 March 2015
Available online 2 April 2015

Keywords:
Li-ion batteries
Cathode material
Special core-shell structure
Lithium manganese phosphate
Lithium vanadium phosphate

ABSTRACT

The energy crisis and energy security leads a great attention to Li-ion batteries (LIB) as the excellent power candidates. We successfully synthesized $LiMnPO_4{\cdot}Li_3V_2(PO_4)_3$/C composite cathode material with high capacity and excellent cycling performance from prickly $MnV_2O_6{\cdot}2H_2O$ precursor, following chemical reduction and lithiation with double carbon sources. The $LiMnPO_4{\cdot}Li_3V_2(PO_4)_3$/C sample has a special multicore-shell structure, whose inner stuffing are $LiMnPO_4$ and $Li_3V_2(PO_4)_3$ in the range of 5-25nm. The initial discharge capacity of $LiMnPO_4{\cdot}Li_3V_2(PO_4)_3$/C composite delivers 221.4 mAh g^{-1}, 202.3 mAh g^{-1} and 152.9 mAh g^{-1} at the rate of 0.1C, 1C and 5C in the range of 1.5-4.5 V, and retains 99.5%, 99.1% and 94.3% of its initial discharge capacity after 50 cycles, respectively.

1. Introduction

Energy storage is more important today than at any time in human history. Future generations of rechargeable lithium batteries are required to power portable electronic devices (cell phones, laptop computers etc.), store electricity from renewable sources, and as a vital component in new hybrid electric vehicles [1]. Li-ion batteries (LIB) have been paid great attention as the excellent candidates. Following the introduction of $LiFePO_4$ by Padhi et al. [2], the strong P-O bonds in the three-dimensional solid framework in $(PO_4)^{3-}$ has been proved to guarantee both the dynamic and thermal stability required to fulfill the safety features in high power applications mentioned above. However, the lower energy density of Li-ion batteries prohibits their further influence in high energy applications [3].

As an alternative approach to improve the energy density, the Fe in $LiFePO_4$ was replaced with other transition-metals, such as Mn, Co, and Ru, to raise the working potential [4]. $LiMnPO_4$ has a theoretical capacity of 171 mAh g^{-1}, and higher Li^+ intercalation potential of 4.1 V versus Li^+/Li (3.4 V for $LiFePO_4$), providing about 20% higher capacity than $LiFePO_4$ for lithium ion batteries.

However, the low electronic conductivity of $LiMnPO_4$ limits its performance at high currents [5]. Monoclinic $Li_3V_2(PO_4)_3$ with PO_4 tetrahedra and VO_6 octahedrain NASICON structure, provides efficient three-dimensional path ways for Li^+ extraction than the one-dimensional pathways in $LiFePO_4$ [6]. Moreover, S Patoux et al. [7] studied the presence of eight (4+4) two-phase domains of $Li_3V_2(PO_4)_3$ in the range of 1.0-4.65 V for charge/discharge. Li is extracted from $Li_3V_2(PO_4)_3$ towards $V_2(PO_4)_3$(V^{4+}/V^{3+} and V^{5+}/V^{4+}couples) through four redox phenomena at 3.59 V, 3.67 V, 4.06 V and 4.35 V. Additionally, $Li_3V_2(PO_4)_3$ shows four reversible redox phenomena upon insertion of two Li^+ (V^{3+}/V^{2+} couple), at 1.98 V, 1.88 V, 1.73 V and 1.70 V. The use of the third electron, conducting to A-$V_2(PO_4)_3$, and the four reversible redox reaction upon insertion of two Li^+(V^{3+}/V^{2+}couple) would increase the capacity equal to $Li[Ni_{0.60}Co_{0.15}Mn_{0.25}]O_2$ [8], but the cycling behavior is not optimized yet.

The dope of $LiMnPO_4$ and uniform particles of nanometer have been proved can improve the electrochemical performances of $Li_3V_2(PO_4)_3$ significantly [9–16]. However, these two method can hardly be combined because the Mn and V can hardly be dispersed through conventional method like ball milling. The uneven distribution of Mn and V will reduce the number of nucleation which will increase the size of particles.

In this paper, we propose a strategy that the nano-sized $LiMnPO_4{\cdot}Li_3V_2(PO_4)_3$/C can combine the two strength by the application of a new special novel prickly $MnV_2O_6{\cdot}2H_2O$. Recently,

* Corresponding author.
E-mail address: huitong@csu.edu.cn (H. Tong).

http://dx.doi.org/10.1016/j.electacta.2015.03.091
0013-4686/

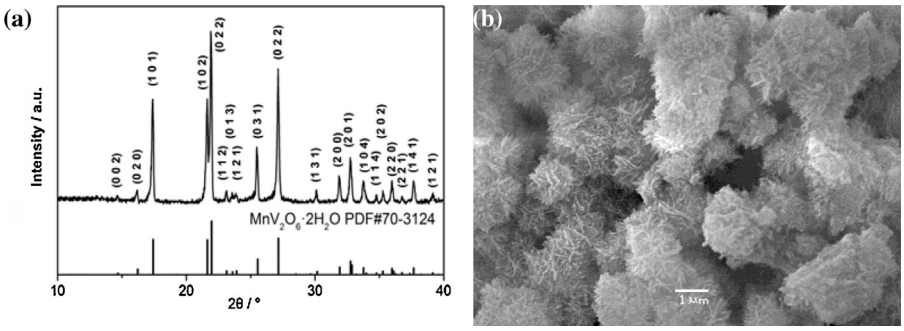

Fig. 1. (a)XRD profiles of $MnV_2O_6{\cdot}2H_2O$ precursor. (b)SEM image of $MnV_2O_6{\cdot}2H_2O$ precursor.

similar rod-like compound was introduced to the $LiMnPO_4{\cdot}Li_3V_2(PO_4)_3$/C cathode by our group to obtain a granular micro-nanosized composite with less ideal electrochemical properties [17]. The precursor has crystallographic structure and the mole ratio of Mn and V matches well with the Mn and V in $LiMnPO_4{\cdot}Li_3V_2(PO_4)_3$/C. The uniform distribution of Mn and V enhance the number of nucleation and reduce the size. Thus, the $LiMnPO_4{\cdot}Li_3V_2(PO_4)_3$/C would possess excellent performance, with the nano-particles and the doping of $LiMnPO_4$.

2. Experimental

2.1. Material synthesis

$MnV_2O_6{\cdot}2H_2O$ was synthesized via the route combined of hydrothermal method and aqueous co-precipitation method [17]. In a typical experiment, the NH_4VO_3 solution (0.01 mol L^{-1}, 0.4L) was dropped into the $Mn(CH_3COO)_2{\cdot}4H_2O$ solution (0.01 mol L^{-1}, 0.2L) with a peristaltic pump with vigorous stirring and ultrasonic dispersion. The pH value of the solution was employed to be adjusted to 7 by using ammonia water after the mixture of two solutions. Small amount of cetyltrimethylammonium bromide (CTAB) was added into the solution. The solution was transferred into a hydrothermal synthesis reactor. Then the reactor was sealed and maintained at 120°C for 4 h and cooled down to room temperature in air. Finally, the brick-red slurry products were filtered, washed several times with distilled water and absolute alcohol to remove ions possibly remaining in the final products, and finally dried at 80°C in air for 4 h. Then the stoichiometric ratio of $MnV_2O_6{\cdot}2H_2O$ precursor, LiH_2PO_4 (99.9 wt.%), oxalic acid were mixed by ball milling for 4 h in alcohol, the oxalic acid is the reducer and also works as carbon source. The resulting mixture was dried at 80°C and subsequently fired in argon atmosphere at the temperature of 700°C for 10 hours. Finally the $LiMnPO_4{\cdot}Li_3V_2(PO_4)_3$/C(marked as LMP·LVP/C) was obtained.

2.2. Characterization

The powder X-ray diffraction (Rint-2000, Rigaku) measurement using Cu Kradiation was employed to identify the crystalline phase of the synthesized materials. The morphology and structure were observed by scanning-electron microscope (SEM, JEOL, JSM-5600LV), energy dispersive X-ray (EDX) detector and a Tecnai G12 transmission electron microscope (TEM). Elemental carbon analysis of the composite was performed by C-S analysis equipment (Eltar, Germany).

2.3. Electrochemical test

The electrochemical characterizations were detected using CR2025 coin-type cell. For positive electrode fabrication, the prepared powders were mixed with 10% of carbon black and 10% of polyvinylidene fluoride (PVDF) in N-methyl pyrrolidinone (NMP) until slurry was obtained. And then, the blended slurries were pasted onto an aluminum current collector, and the electrode was dried at 120°C for 4 h in the air with an average mass of 2-2.5 mg·cm^{-2} of active material for a disk of diameter 14 mm. The counter electrode was a disk of lithium metal. The electrolyte was a 1 mol L^{-1} solution of $LiPF_6$ in EC, EMC and DMC (1:1:1 in volume). A porous polypropylene film was used as a separator. The assembly of the cells was carried out in a dry Ar-filled glove box. Electrochemical tests were carried out using an automatic galvanostatic charge-discharge unit, NEWARE battery cycler, between 1.5-4.5 V versus Li/Li^+ electrode at room temperature.

3. Results and discussion

The XRD pattern of $MnV_2O_6{\cdot}2H_2O$ precursor is shown in Fig. 1. All peaks are indexed on the basis of the data of JCPDS#70-3124, space group Pnma62. The crystal structure is identified to be orthorhombic structure, which is consistent with that reported by JOËL [18]. Fig. 2 shows the SEM image of the $MnV_2O_6{\cdot}2H_2O$. Homogeneous precursor with special prickly morphology can be observed in the image. Moreover, the Mn/V mole ratio of $MnV_2O_6{\cdot}2H_2O$ is 2.007 based on analysis of chemical titration, confirming that the prepared brick-red precipitate is $MnV_2O_6{\cdot}2H_2O$.

Fig. 3 shows the XRD and Rietveld refinement XRD pattern of LMP·LVP/C. All diffraction peaks can be clearly indexed to the orthorhombic $LiMnPO_4$ phase (space group Pnma, 25834-ICSD) and monoclinic $Li_3V_2(PO_4)_3$ phase(space group P21/n, 96962-ICSD). The refined lattice parameters and phase content are listed in Table 1. The observed and calculated patterns match well, and the reliability factor (R_w) is acceptable. The data indicates that the cell volume of $LiMnPO_4$ in the LMP·LVP/C composites decreases, compared with the pure orthorhombic $LiMnPO_4$, which may attribute to the V doping on the Mn sites because of smaller ionic

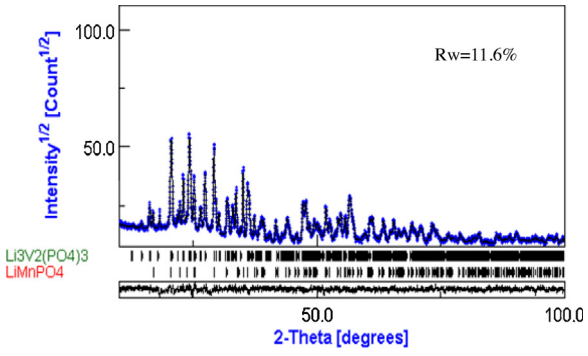

Fig. 2. Rietveld refinement XRD patterns of LVP·LMP/C composites.